

A Novel Technique for Compensating the Harmonics in An Active Harmonic Filter Based on one Cycle Control Theory

B. HARIKA (PG Scholar)¹

M. SAIDA RAO (Ph.D)²

¹*Department of EEE, AVANTHI'S SCIENTIFIC TECHNOLOGICAL & RESEARCH ACADEMY, JNTU (HYD)*

²*Assistant Professor, AVANTHI'S SCIENTIFIC TECHNOLOGICAL & RESEARCH ACADEMY, JNTU (HYD)*

Abstract- during this paper we have a tendency to planned a sophisticated topology for load compensators for concluding harmonic and reactive power compensation with the assistance of symbolic logic controller. Hence, it's customary to use active harmonic filters for harmonic compensation solely, whereas ancient strategies comprising of thyristor-switched capacitors ar accustomed do reactive power compensation. so as to beat the same limitation, associate degree OCC-based shunt harmonic filter that symbolic logic controller given here it is capable of compensating solely the harmonic elements of the load current is planned during this paper. The viability of the planned theme is confirmed by performingand the MATLAB/SIMULINK model is given here together with results.

Index Terms—Fuzzy logic controller (FLC),Active power filters, harmonic filters, one-cycle control (OCC).

I.INTRODUCTION

A shunt load compensator provides the harmonic current demand of the nonlinear load connected in parallel with the compensator and to boot provides reactive power support for power issue correction and/or voltage regulation. fashionable active load compensators have higher filtering performance and smaller physical size compared to passive harmonic filters and may be used for a range of power quality improvement applications. because the load compensator provides the reactive part of the load current in conjunction with harmonics, it's needed to be rated to hold the reactive part of the load current conjointly. Moreover, the high information measure demand of the controller that forces the compensator to provide the harmonic part of the load current necessitates the semiconductor switches to work at high change frequencies.

Operation of semiconductor devices at high change frequency whereas they carry massive current results

in increment in device current rating and change losses.The magnified rating makes the load compensators big-ticket. so as to beat the said limitation, compensators square measure controlled such they Act as active harmonic filters (AHFs) to compensate just for the harmonic elements of the load current, whereas ancient strategies comprising of thyristor switched Capacitors/reactors square measure wont to perform reactive power compensation of the given load. because the shunt AHF Connected in parallel with a nonlinear load compensates just for the harmonics generated by the load, the utility views the mixture of nonlinear load and AHF as a linear load. what is more, because the convertor of associate degree AHF needs to carry solely the harmonic elements of the load current, its current rating and also the incurred power loss square measure less compared thereto of a load compensator.

Typically, the harmonic extractor of associate degree AHF determines the harmonic elements of the load current and thereby sets this reference for the harmonic filter. The common strategies used for harmonic extraction in three-phase AHFs square measure the fast active and reactive power (p-q) technique , synchronous organisation (d-q) technique , fast active and reactive current part technique , strategies derived from fast reactive power theory , notch filter-based strategies, and Kalman-filter-base technique . Once the harmonic current reference is generated, the filter current is forced to follow the set current reference with the assistance of a high information measure current controller.

A linear current controller, a exhausted controller, or a physical phenomenon controller are often used for this purpose. All of those strategies need the knowledge of the basic part of the grid voltage to extract the harmonics gift within the supply current. The grid voltage is probably going to contain distortions, together with multiple zero crossings, and



also the service of a phase-locked loop (PLL) is used to extract the basic part of the grid voltage. The presence of distortions and deviations within the grid voltage makes the look of PLL and its implementation computationally intensive and creates further burden on the microcontroller/digital signal processor concerned. What is more, a number of the said current management strategies operate with variable change frequency that reduces the effectiveness of the magnetic attraction interference (EMI) filter.

One-cycle-controlled converters, in general, and cargo compensators supported one-cycle management (OCC) don't expressly need part and frequency data of the grid voltage, and hence, they'll be enforced while not the service of a PLL. The absence of PLL in OCC-based schemes makes them strong and conjointly ensures that they'll be accomplished by using straightforward analog circuits. Moreover, during this case, semiconductor devices operate at constant change frequency, that makes the look of the EMI filter easier. Additionally, the dynamic performance of the OCC-based converter is best owing to the presence of inner current loop and since of the actual fact that it's enforced mistreatment analog devices.

In principle, analog management techniques have the quickest response owing to their continuous corrective action not late by the analog-to-digital conversion method or delays introduced as a fall out of the existence of the computation time. However, the OCC-based load compensators given in cannot differentiate between the reactive part and harmonic elements of the load current. The parallel combination of the OCC-based load compensator and also the nonlinear load poses as associate degree emulated resistance to the grid, and its management strategy ensures that the grid current follows the grid voltage. Hence, the utility grid finishes up provision solely the \$64000 part of the load current and also the flexibility to work the compensator solely as associate degree AHF isn't doable.

The said downside of the OCC-based compensator is self-addressed by a three-phase load compensator given during which relies on point in time balance (PAB) management. This load compensator supported OCC has the flexibleness to provide the harmonic elements of the load and/or reactive power of the load betting on the need of the appliance. The comparatively straightforward management structure of the PAB technique is employed to extract the harmonic part of the load current. The management loop has no current error amplifiers or observers, that square measure usually needed for estimation of the input voltages.

Moreover, the comparatively straightforward management structure of the harmonic extractor doesn't take into thought the problems concerned within the implementation of the high information measure current controller needed to force the filter current to follow the reference current.

during this paper, associate degree OCC-based compensator in conjunction with FLC that operates as associate degree AHF, thereby compensating just for the load harmonics is projected. This basic philosophy of the projected theme is bestowed in [21]. Not like different OCC-based load compensators that square measure offered within the literature, the OCC-based AHF projected during this paper carries out partial compensation (harmonics alone) whereas retentive the foremost blessings of OCC-based load compensators gift within the literature. So as to check the OCC-based compensators with different existing harmonic extraction techniques and current management schemes reported within the literature [6]–[10], the capabilities and necessities of varied schemes square measure summarized in Table I. It's evident from Table I that OCC-based schemes square measure straightforward to implement compared to different schemes. All different schemes have the constraint of procedure burden needed in implementing the PLL and conjointly in realizing the coordinate or domain transformations needed to extract the harmonic data. Conventional current controllers have the matter of variable change frequency (hysteresis controller) and slow response (linear controller). OCC-based managementers operate at constant change frequency and conjointly exhibit a quick dynamic response because the current control loop is embedded within the PWM modulator having a dynamic response determined by the speed of change cycles. What is more, the theme projected during this paper doesn't have the constraints encountered by the OCC-based AHF bestowed.

II. PROPOSED ONE-CYCLE-CONTROLLED AHFS

In order to understand the principle of operation of the proposed OCC-based AHF, first the basic working philosophy of the OCC-based load compensator presented in and is briefly explained. The schematic power circuit diagrams of the shunt load compensator system compensating single phase and three-phase nonlinear loads are shown in Fig. 1(a) and (b), respectively. The control goal of the OCC-based load compensator described in , which is used to compensate for the nonlinear loads of the system shown in Fig. 1(a), is to satisfy the following relationship:

$$i_s = v_s / R_e \quad (1)$$

where v_s , i_s , and R_e represent the grid voltage at the point of common coupling, the current drawn from the grid, and the emulated resistance of the parallel combination of the load compensator and the nonlinear load as seen by the grid, respectively. In case of the three-phase system, v_s and i_s represent the per-phase equivalent voltage and the corresponding current, respectively.

The block diagrams of the controller of the aforementioned single-phase OCC-based load compensator presented in [14] is shown in Fig. 2. The dc link voltage V_{dc} is sensed and compared with the reference dc link voltage to generate the error between the controlled and reference functions. A PI controller processes this error signal to generate a reference signal V_m . A symmetrical sawtooth waveform whose peak is equal to that of the reference signal V_m is generated using an integrator with a reset and an adder, as shown in Fig. 2. This sawtooth waveform serves as the carrier signal which is used to generate the pulsewidth modulated signals to be delivered to the gates of converter switches. A free-running clock having a time period T_s is used to reset the integrator, and hence, the frequency of the clock $T_s - 1$ decides the frequency of the sawtooth waveform and hence the switching frequency of the devices. The time constant of the integrator T_i is chosen to be half of T_s as explained in [14].

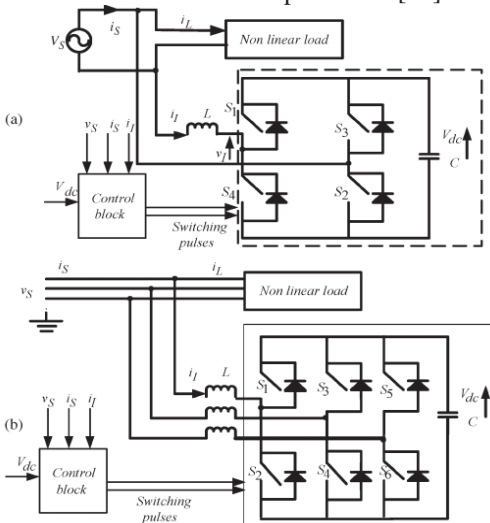


Fig.1. Schematic block diagram of single- and three-phase shunt AHF systems.

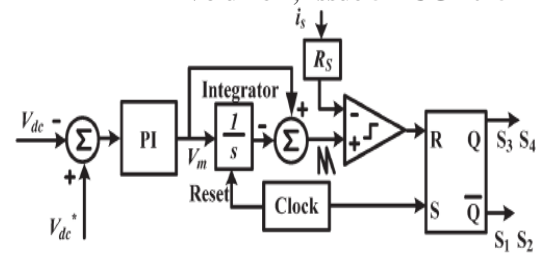


Fig.2. Block diagram of the controller for the conventional single-phase OCC-based load compensator system.

The grid current is sensed by a current sensor having gain R_s to obtain the modulating signal x so that

$$X = i_s R_s \quad (2)$$

The modulating signal is compared with the carrier sawtooth waveform. The output of this comparator is used to reset a set–reset (SR) flip-flop, which is set at every rising edge of the free-running clock. The output of the SR flip-flop serves as switching pulses for the converter. The process of generation of switching pulses by comparing a typical modulating signal with a sawtooth carrier signal is illustrated in Fig. 3. When the modulating signal x is less than the sawtooth waveform, S_3 and S_4 are turned on, thereby making the output voltage of the converter to be $-V_{dc}$. When x is greater than the sawtooth waveform, S_1 and S_2 are turned on, and the output voltage of the converter is $+V_{dc}$. Assuming that the modulating signal x remains constant within the switching period, the average output voltage of the converter during a switching time period or the time period of the sawtooth waveform is

$$v_1 = \frac{V_m - x}{2V_m} (-V_{dc}) + \frac{V_m + x}{2V_m} (V_{dc}) = \frac{V_{dc}}{V_m} x \quad (3)$$

It can be inferred from (3) that the average converter output voltage in a switching time period is proportional to the modulating signal x . The output voltage of the converter averaged over a switching time period can be obtained by combining (2) and (3) as follows:

$$v_1 = V_{dc} R_s / V_m i_s = K i_s \quad (4)$$

From (4), it can be inferred that the output voltage of the converter averaged over a switching period is proportional to the source current. Therefore, the converter can be modeled as a current-controlled voltage source, and the equivalent circuit of the load compensator depicted in Fig. 1 can be modeled as shown in Fig. 4(a). The fundamental component of the grid voltage at the point of common coupling (V_{s1}), the fundamental component of the converter output voltage (V_{11}), the fundamental

$$I_{1h} = V_{1h}/j h L \omega = K I_{sh}/j h L \omega \quad (10)$$

component of the current drawn from the grid (I_{S1}), the fundamental component of the inverter current (I_{I1}), and the fundamental component of the load current (I_{L1}) are also shown in Fig. 4(a). As the dc link voltage is maintained at a value equal to the set reference and if losses in the system are neglected, real power negotiated by the converter is zero. If the grid voltage is assumed to be distortion less, the expression for the real power supplied by the converter when the system is assumed to be lossless is given in (5), where δ is the angle between the fundamental component of the converter output voltage and the grid voltage

$$P = V_{11} V_{S1} \sin \delta / \omega L = 0 \quad (5), \quad \delta = 0$$

From (4) and (5), it can be inferred that the following three are in phase with each other: 1) the fundamental component of the converter output voltage (V_{I1}); 2) the current supplied by the grid (I_{S1}); and 3) the grid voltage (V_{S1}) at the point of common coupling. The phasor diagram of the system is shown in Fig. 5. Since the fundamental component of the grid voltage and the current drawn from the grid are in phase, no reactive power is supplied by the grid, and the entire reactive power requirement of the load Q is supplied by the converter, which can be expressed as

$$Q = V_{I1} V_{S1} \cos \delta - V_{S1}^2 / \omega L = 0 = \frac{(V_{I1} - V_{S1}) V_{S1}}{\omega L} \quad (6)$$

The real power required by the load P is supplied by the grid and is given by

$$P = V_{S1} I_{S1} \quad (7)$$

Combining (4), (6), and (7), K can be expressed as

$$K = (Q_{wl} + V_{S1}^2) / P \quad (8)$$

In order to find the efficacy of the conventional OCC based load compensator to compensate for the higher order harmonic currents drawn by the nonlinear load, the equivalent circuit of the load compensator system for the h_{th} harmonic order components is deduced from Fig. 4(a) and is shown in Fig. 4(b). Using (4), the h_{th} order harmonic component of the converter output voltage V_{Ih} is proportional to the h_{th} order harmonic component of the source current I_{Sh} , which is expressed as

$$V_{Ih} = K I_{Sh} \quad (9)$$

Using the equivalent circuit of Fig. 4(b), the converter current of the h_{th} order harmonics (I_{Ih}) is given as

Applying Kirchhoff's current law at node A of Fig. 4(b)

$$I_{Sh} + I_{Ih} = I_{Lh} \quad (11)$$

Combining (10) and (11)

$$I_{Sh} = I_{Lh} / (1 - jK/hL\omega) \quad (12)$$

From (12), it can be inferred that the capability of the load compensator system to perform harmonic compensation for a load current of a particular harmonic component h depends on the value of K , which is a function of the real and reactive power demand of the load as given in (8). To achieve effective compensation, the harmonic current drawn from the grid should be as small as possible, and to realize that, K_{hoL} . Therefore, from (8), the condition for effective compensation of the h_{th} order harmonic of the load current can be expressed as

$$L \ll V_s^2 / \omega (P_h - Q) \quad (13)$$

It is evident from (4) and the phasor diagram of Fig. 5 that the grid current i_s is in phase with the grid voltage and the reactive power requirement of the nonlinear load is not supplied by the grid. The aim of the controller of the proposed OCC-based AHF is to relieve the burden of supplying the reactive power requirement of the load from the converter. The control goal of the proposed AHF has to be modified such that the utility grid sees the parallel combination of the AHF and the nonlinear load as equivalent impedance

It is evident from (4) and the phasor diagram of Fig. 5 that the grid current i_s is in phase with the grid voltage and the reactive power requirement of the nonlinear load is not supplied by the grid. The aim of the controller of the proposed OCC-based AHF is to relieve the burden of supplying the reactive power requirement of the load from the converter. The control goal of the proposed AHF has to be modified such that the utility grid sees the parallel combination of the AHF and the nonlinear load as an equivalent impedance

$$i_{cref} = \int v_s dt / L_e \quad (14)$$

where L_e is the emulated inductance of the AHF system. The reactive current reference so obtained is subtracted from the source current and is scaled to get the modulating signal x , where

$$X = (i_s - i_{cref})R_s \quad (15)$$

Combining (3) and (15), the expression for the converter output voltage v_l , averaged over a switching time period, is obtained as follows

$$v_1 = \frac{V_{dc} R_s}{V_m} (i_s - i_{cref}) = K (i_s - i_{cref}) \quad (16)$$

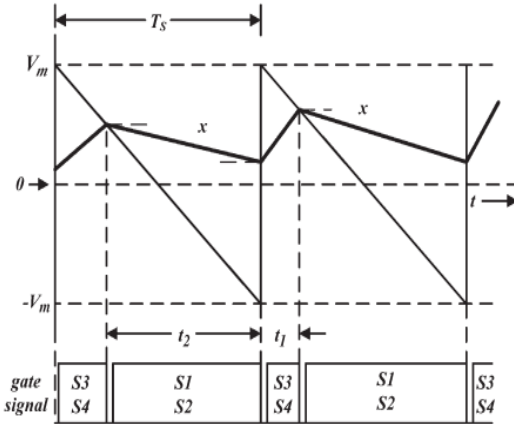


Fig.3. Carrier waveform (saw tooth), modulating waveform x , and gating signal.

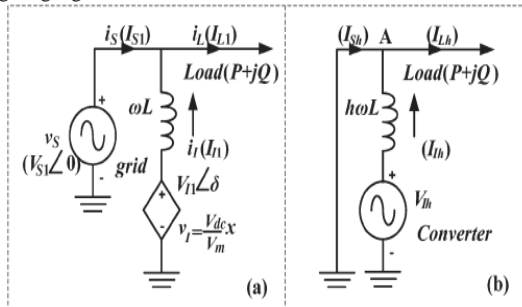


Fig.4. Equivalent circuit of the (a) fundamental harmonic of the filter system and (b) h th harmonic of the filter system ($h > 1$)

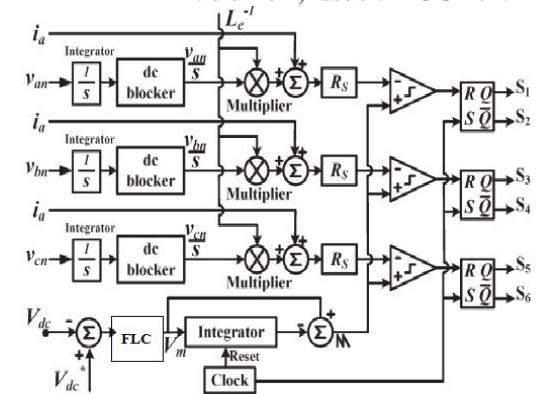
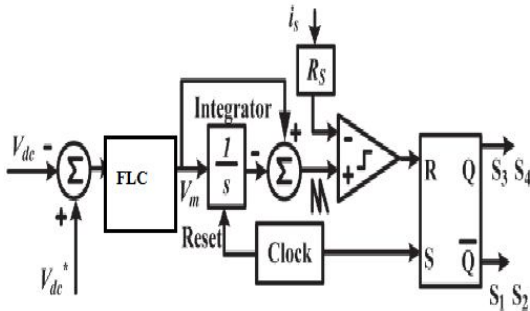


Fig.5. Block diagram of the controller for the proposed OCC-based AHF.
(a) Single-phase system. (b) Three-phase system.

It can be inferred that the converter output voltage, averaged over a switching period, is proportional to the sum of the grid current and the reactive current reference. The reactive current reference ensures that there is a phase shift between the fundamental component of the grid current and converter output voltage. However, the converter output voltage is in phase with the grid voltage as the closed-loop controller ensures that there is no real power flow between the grid and the converter by maintaining the dc link voltage constant, which has already been explained earlier. This implies that there is a phase shift between the grid voltage and the grid current. Hence, the governing control equation of the proposed OCC-based AHF system can be stated as

$$I_s = V_s / (R_e + j\omega L_e) \quad (17)$$

Here, R_e is the emulated resistance, and L_e is the emulated inductance as seen by the utility grid due to the parallel combination of the load compensator and the nonlinear load. Furthermore, from the block diagram of the controller given in Fig. 5, it can be seen that the control structure has two loops, namely, a fast inner control loop and a slow outer control loop. The inner loop maintains the dc link voltage at the set reference point so that the net power negotiated by the converter is only the losses incurred in the compensating system. The detailed structure of the outer loop is given in Fig. 6. It sets the reactive current reference by determining the value of the emulated inductance as seen by the source. The numerical value of the emulated inductance can be either positive or negative depending on the leading or lagging nature of reactive current demand of the load.

The converter current i_l is sensed and is controlled in such a way that the peak of the

fundamental component of the converter current I_{l1peak} is equal to a small set reference I_{l1}^*peak . The sensed converter current is passed through a band pass filter and a peak detector to determine the peak of the fundamental component of the converter current I_{l1peak} . Ideally, the reference for the amplitude of the fundamental component of the converter current I_{l1}^*peak should be set to zero, but due to certain practical constraints, it is set to a low value, nearly equal to zero. These constraints arise mainly due to the following reasons: 1) the fundamental component of the converter current cannot become zero, because it has to supply the loss incurred in the compensating system; and 2) the output of the second-order band pass filter which is employed to extract the fundamental component of the converter current cannot assume a zero value, as the converter current contains higher order harmonics that cannot be completely filtered out.

The sensed converter current i_l is filtered using the second order bandpass filter to obtain the fundamental component of the current i_{l1} . A free running clock, CLK2, produces pulses at frequency near to 45 Hz, which is slightly lower than supply frequency (50 Hz). CLK2 is used to reset the peak detector which determines the peak of the fundamental component of the converter current I_{l1peak} . A sample-and-hold circuit, triggered by the free-running clock CLK2, is used to hold the value of the peak of the converter current in the previous cycle $I_{l1peak}(n-1)$. The error between I_{l1peak} and I_{l1}^*peak (ΔI_{l1peak}) is used to determine the value of the emulated inductance. This decision has to be taken based on the information whether the utility is sourcing a lagging or leading current.

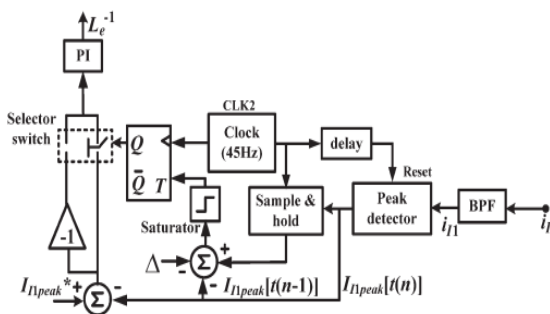


Fig.6. Schematic block diagram of the feedback loop which sets the value of the emulated inductance.

FUZZY LOGIC CONTROLLER

THE FUZZY LOGIC CONTROLLER

Fuzzy logic control is a non-mathematical decision algorithm that is based on an operator's

experience. The fuzzy logic controller can easily be programmed to handle this region.

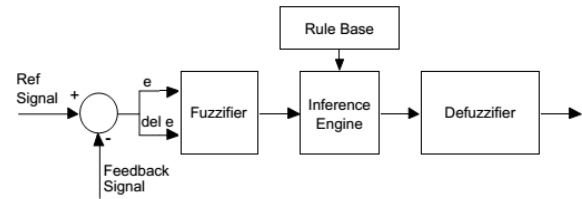


FIG 7 Structure of Fuzzy Logic Controller
FUZZIFIER

Fuzzy logic uses linguistic variables instead of numerical variables. In a closed loop control system, the error (e) between the reference voltage and the output voltage and the rate of change of error (del e) can be labeled as zero (ZE), positive small (PS), negative small (NS), etc. In the real world, measured quantities are real numbers (crisp). The process of converting a numerical variable (real number) into a linguistic label (fuzzy number) is called fuzzification. Figure shows the membership functions that are used to fuzzify the inputs.

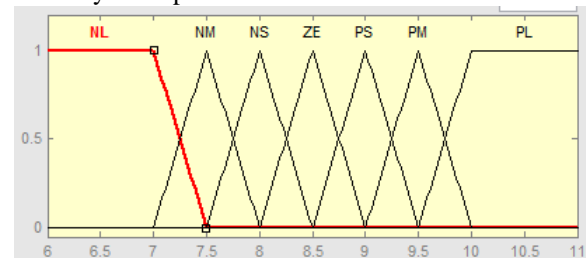


Fig 8 Input1 membership functions

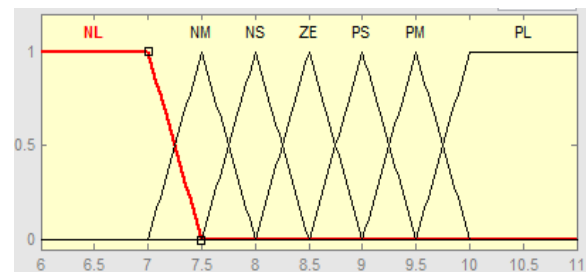


Fig 9 Input2 membership functions

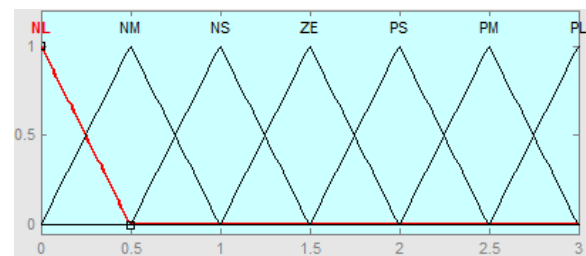


Fig 10 output1 membership functions



The inputs are mapped into these membership functions and a degree of membership is found for how much the input belongs to that particular linguistic label. The membership can take on a value from zero to unity for each of the linguistic labels. The waveforms are evenly distributed about the range of operation of the variables. For each of the input and output variables, the following seven linguistic labels are assigned to the membership functions:

- NL = Negative Large
- NM = Negative Medium
- NS = Negative Small
- ZE = Zero
- PS = Positive Small
- PM = Positive Medium
- PL = Positive Large

Once the membership is found for each of the linguistic labels, an intelligent decision can be made unto what the output should be. This decision process is called inference.

Table I
 Fuzzy logic rules

INFERENCE

In conventional controllers, there are control laws, which are combinations of numerical values that govern the reaction of the controller. In fuzzy logic control, the equivalent term is rules. Rules are linguistic in nature and allow the operator to develop a control decision in a more familiar human environment [4]. A typical rule can be written as follows: If the “voltage” is negative large (NL), AND the “rate of change of voltage error” is negative large (NL), then the “field current” is positive large (PL). In this design, a minimum correlation inferencetechnique was used. This means that the logic

membership that was equal to the minimum of the two inputs, voltage – NLand rate of change of voltage – NL. For example

$$\text{Membership (V – NL)} = .8 \quad \text{Membership (del V – NL)} = .2$$

$$(.8) \text{ AND } (.2) = .2$$

operation of AND will return the minimum of all inputs. For the linguistic rule stated earlier, the output, field current - PL, would receive aThe rules of a fuzzy logic controller give the controller its intelligence, assuming the rules are developed by a person who has a experience with the system to be controlled.

A programmer with more experience with the system will create a better controller. In the case of the fuzzy logic synchronous generator controller, the

desired effect is to keep the output voltage of the generator at its rated voltage under varying loads. From this desired goal, rules are made for every combination of voltage and rate of change of voltage on what the field currentshould be in order to stabilize the generator. It is convenient when dealing with a large number of combinations of inputs, to put the rules in the form of a rule table. Figure 6 shows the rule table for controlling the synchronous generator output voltage where Del Voltrefers to the rate of change of output voltage.After the rules are evaluated, each output membership function will contain a corresponding membership. From these memberships, a numerical (crisp) value must be produced. This process is called defuzzification.

DEFUZZIFICATION

Defuzzification plays a great role in a fuzzy logic based control system. It is the process in which the fuzzy quantities defined over the output membership functions are mapped into a non-fuzzy (crisp) number. It is impossible to convert a fuzzy set into a numeric value without loosing some information. Many different methods exist to accomplish

e\de	NL	NM	NS	ZE	PS	PM	PB
NL	PL	PL	PL	PL	PM	PS	ZE
NM	PL	PL	PM	PM	PS	ZE	NS
NS	PL	PM	PS	PS	NS	NM	NL
ZE	PL	PM	PS	ZE	NS	NM	NL
PS	PL	PM	PS	NS	NS	NM	NL
PM	PM	ZE	NS	NM	NM	NL	NL
PL	ZE	NS	NM	NL	NL	NL	NL

defuzzification. Naturally there are trade-offs to each method.

A selector switch selects either $\Delta I/I_{peak}$ or $-\Delta I/I_{peak}$ before it is passed on to the PI regulator. The selector switch iscontrolled by a toggle flip-flop, whose output will toggle if thepeak of the fundamental component of the inverter current hasincreased compared to that of the previous sampling instant,i.e., if $I/I_{peak} > I/I_{peak}(t(n - 1))$. The toggling of the flipflop will change the selection of the selector switch, and the appropriate signal (error or its inverse) is fed to the PI controller.The output of this PI regulator determines the magnitude of theemulated inductance L_e

When there is an abrupt change in reactive power requirement of the load, the AHF will tend to supply the difference in reactive power during the transient period as the control loop for generating the reactive current reference is much slower than the inner loop that maintains the dc link voltage. This

$$P = V_{S1} I_{S1} \cos \phi \quad (18)$$

leads to a sudden increase in current during the transient period which may exceed the rating of the switching devices. In order to overcome this problem, a current limiter, shown in Fig. 8, is incorporated in the controller to limit the current to a maximum permissible value during the transient duration. The converter current is compared with the threshold value set for the current limiter. If the current is above the threshold level, the SR flip flop is reset, thereby forcing the converter current to fall, even if the modulating signal has not intersected the saw tooth waveform. If the converter current is less than the lower threshold, the SR flip-flop is set, forcing the inverter current to rise. Thus, the current limiter ensures that the converter current does not exceed the current rating at all operating conditions. Since the current limiting is a nonlinear process, the current drawn from the grid gets distorted when the current limiter is in operation.

From Fig. 12

$$\cos \phi = V_{S1} / K I_{S1} \quad (19)$$

Combining (18) and (19), the value of K can be expressed as

$$K = V_{S1}^2 / P \quad (20)$$

It can be noted that (20) is a special case of (8), wherein the reactive power supplied by the converter Q is equal to zero. As given in (12), the capability of the AHF system to perform harmonic compensation for a load current of a particular harmonic component h depends on the value of K , which is a function of the real power demand of the load as given in (20). To achieve effective compensation, the harmonic current drawn from the grid should be as small as possible, and to realize that, $K \gg h_{\omega L}$. Hence, from (20), the condition for effective compensation of the h_{th} order harmonic of the load current can be expressed as

$$L \ll V_s^2 / \omega P h \quad (21)$$

The numerical value of L has to be chosen such that (21) is satisfied, with P being equal to the rated power of the nonlinear load and h being the harmonic order of the load current up to which all harmonics are intended to be compensated.

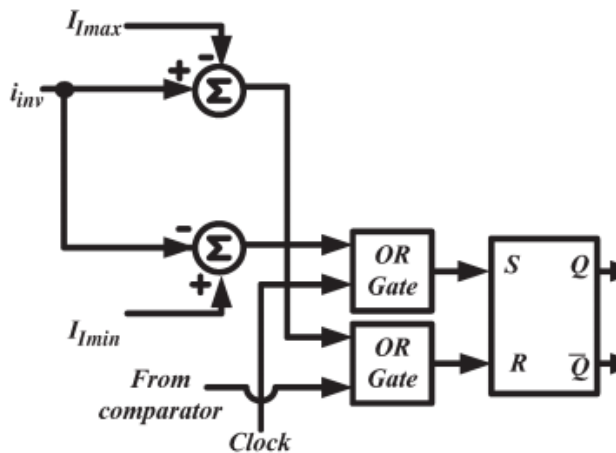


Fig11. Schematic circuit diagram of the current limiter.

In line with the analysis done earlier in this paper, the proposed AHF is also analytically evaluated in terms of its efficacy to compensate for a particular harmonic component of the load current. Since the fundamental component of the converter current is maintained at zero by the closed-loop control, the real and reactive power due to the fundamental component of current supplied by the harmonic compensator is zero. Therefore, the fundamental component of the output voltage of the converter is equal to the grid voltage in magnitude and phase, which is depicted in the phasor diagram given in Fig.12. The fundamental component of the nonlinear load current (I_{L1}) is equal to the grid current (I_{S1}), and therefore, both of these currents are equal in magnitude and phase. The real power supplied by the grid is given by

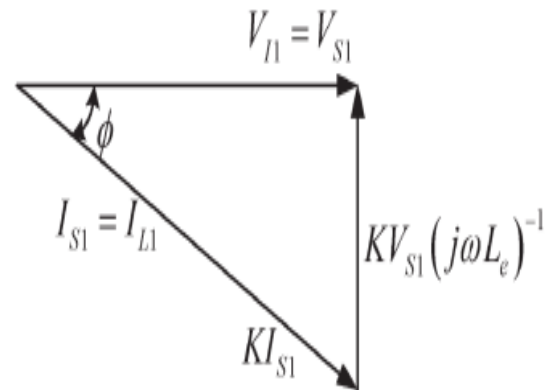


Fig12. Phasor diagram showing the steady-state behavior of the proposed OCC-based shunt AHF system

SIMULATION RESULTS

In order to predict the performance of the proposed OCC-based three-phase shunt AHF system, detailed simulation studies are carried out on

MATLAB–Simulink platform. The parameters of the system chosen for the purpose of simulation are shown in Table II. The steady-state response of the system while compensating the parallel combination of a lagging linear load and a full bridge rectifier load, the details of which are given in Table II, is shown in Fig. 13. It can be inferred from Fig. 13 that the reactive power requirement of the load is supplied by the grid as the grid current lags the grid voltage and the converter current contains harmonic components of the load current only. The harmonic spectra of the load current and the grid current are given in Fig. 14. From the harmonic spectra, it can be noted that all of the low-order harmonics are considerably attenuated. As the controller of the proposed scheme requires information of instantaneous utility voltages, it may appear that distortions present in the utility voltages may affect the operation of the proposed AHF.

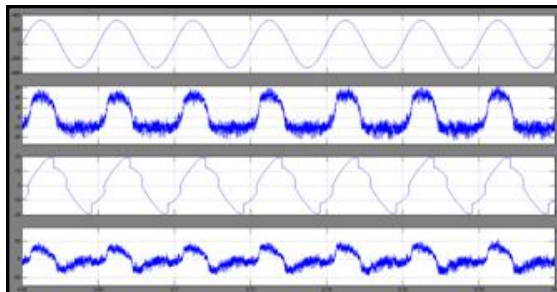


Fig. 13. Simulated steady-state performance of the proposed three-phase OCC-based AHF. (a) Phase-A grid voltage ($v_{S a}$; 200 V/div). (b) Phase-A grid current ($i_{S a}$; 20 A/div). (c) Load current ($i_{L a}$; 20 A/div). (d) converter current ($i_{I a}$; 5 A/div). Time scale: 10 ms/div.

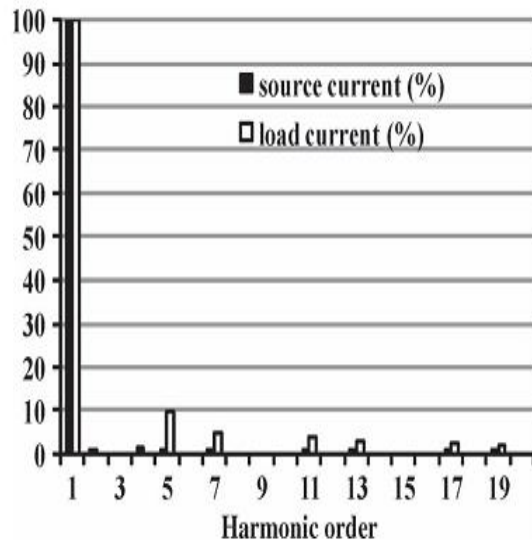


Fig. 14. Harmonic spectra of the load current and the grid current after compensation (simulation studies).

The steady-state performance of the compensator which experiences this situation is emulated by deliberately adding certain harmonic components in the utility voltages. The distortion voltage components that are added to the utility voltages are fifth- and seventh-order harmonic components having magnitudes of 4% and 3% of the fundamental component, respectively. Furthermore, a 5-kHz signal with an amplitude of 40 V is also added to the source so that there are multiple zero crossings in the utility voltage in every power cycle. This simulated performance of the compensator while being fed by the aforementioned distorted grid voltage is depicted in Fig. 15. It can be noted that the compensator operation remains unaffected even in the presence of multiple zero crossings in phase voltages of the source. The harmonic spectra of the load current and the grid current under distorted grid voltage condition are shown in Fig. 16. By comparing the harmonic spectra of Fig. 16 with those of Fig. 14, it can be noted that the harmonics that are present in the grid voltage also make their appearance felt in the current drawn from the utility. This is consistent with the fact that the combination of the OCC-based AHF and the load that is being compensated poses as an emulated impedance to the source.

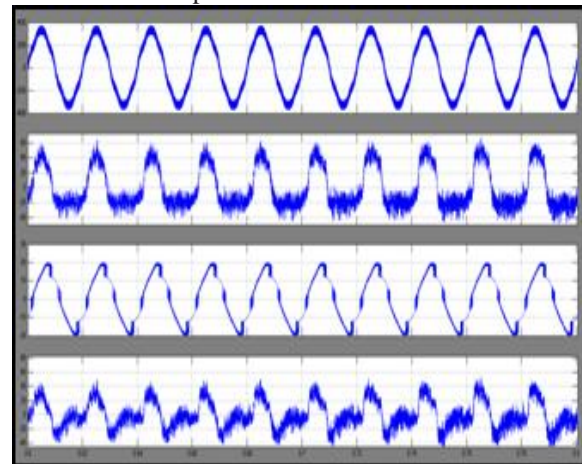


Fig. 15 Simulated steady-state performance of the proposed three-phase OCC-based AHF under distorted voltage conditions. (a) Phase-A grid voltage ($v_{S a}$; 200 V/div). (b) Phase-A grid current ($i_{S a}$; 20 A/div). (c) Load current ($i_{L a}$; 20 A/div). (d) converter current ($i_{I a}$; 5 A/div). Time scale: 10 ms/div.

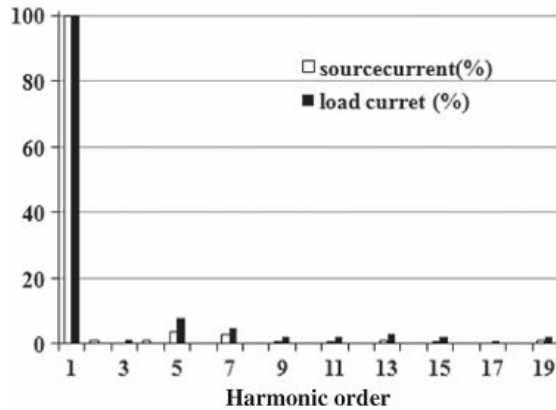


Fig.16. Harmonic spectra of the load current and the grid current under distorted grid voltage conditions (simulation studies)

In order to demonstrate the effect of the current limiter, the simulated performances of the system in the absence and presence of the current limiter are also shown in Fig. 17. The grid current and the converter current when the current limiter is not included in the circuit are depicted in Fig. 17(c) and (d), respectively, while Fig. 17(e) and (f) depicts the grid current and converter current when the current limiter is included in the circuit

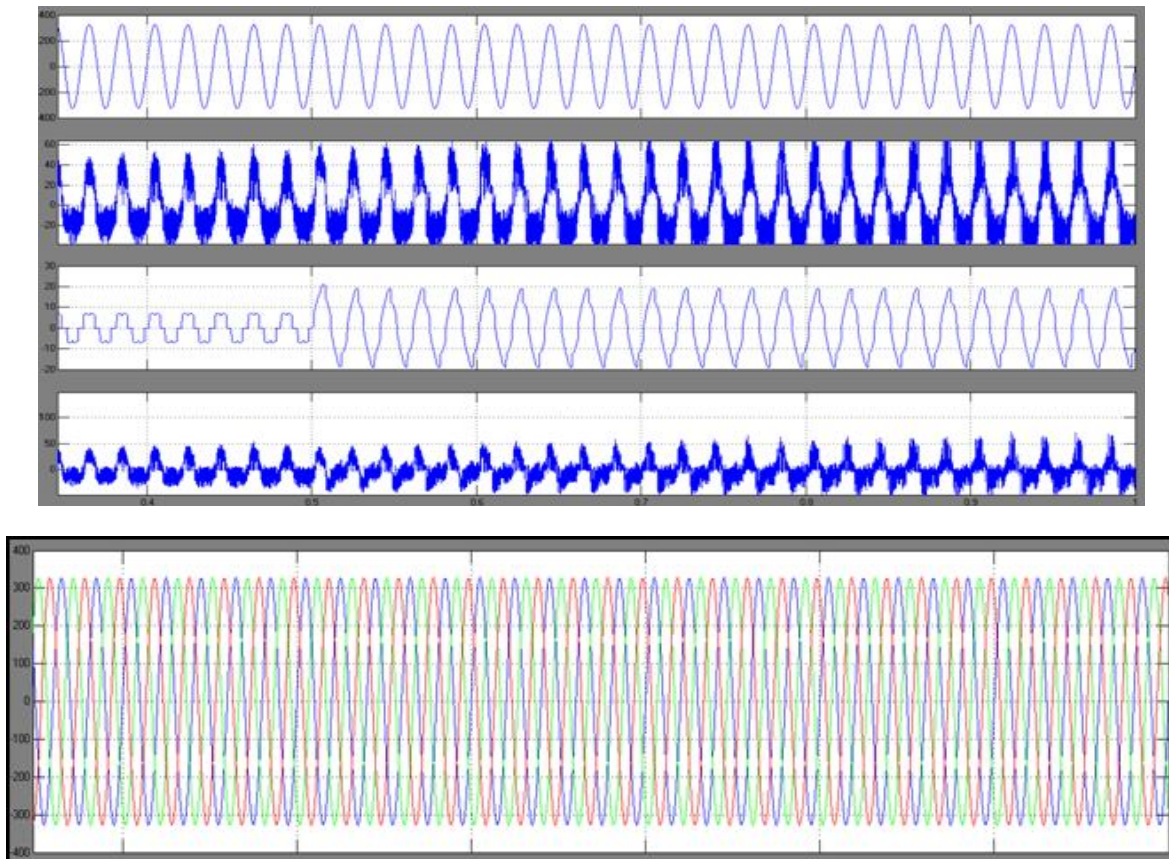


fig 17. Measured performance of the proposed three-phase OCC-based AHF during a sudden change in load. a Source voltage b. source current c. load current d. load voltage e. icabcf

During a step change in the reactive power requirement of the load, the AHF tends to supply the reactive power requirement of the load. Consequently, the converter current tends to increase beyond its rated value, and this can be observed from the converter current waveform shown in Fig. 17(d). When the converter current exceeds the set value of the current limit, the current limiter acts and limits the

current supplied by the converter to the set value, and it can be observed that the grid current gets distorted during this duration, when the current limiter is in action. The activity of the current limiter is limited to a few power cycles, and as the converter current falls below the set current limits and as steady state is reached, the AHF starts supplying only the harmonic components of the load current as is evident from Fig. 17(f).



CONCLUSION

The wide unfold usage of load compensators is restricted as a result of they're pricey and lossy, particularly once it's utilized for reactive power compensation in conjunction with harmonic compensation. Therefore, they're typically controlled to be used as AHFs to compensate solely the harmonic elements of the load current, whereas ancient ways arwont to do reactive power compensation of the given load. Existing OCC based mostly load compensators, that don't need the service of a PLL to urge itself interfaced with the utility grid, can not be utilized for harmonic compensation alone as they find yourself compensating for reactive current in addition. This results in a rise within the rating of the device. so as to beat the same limitation of the OCC-based load compensator, associate degree OCC-based shunt harmonic filter that is capable of compensating solely the harmonic elements of the load current is projected during this paper. With the assistance of analytical studies, elaborate numerical simulation, and experimental verification on a laboratory model, the effectivity of the projected theme has been incontestable .

REFERENCES

[1] H. Akagi, "Active harmonic filters," *Proc. IEEE*, vol. 93, no. 12, pp. 2128–2141, Dec. 2005.
[2] S. Rahmani, A. Hamadi, K. Al-Haddad, and L. A. Dessaint, "A combination of shunt hybrid power filter and thyristor controlled reactor for power quality," *IEEE Trans. Ind. Electron.*, vol. 61, no. 5, pp. 2152–2164, May 2014.
[3] H. Akagi, Y. Kanazawa, and A. Nabae, "Instantaneous reactive power compensators comprising switching devices without energy storage components," *IEEE Trans. Ind. Appl.*, vol. IA-20, no. 3, pp. 625–630, May 1984.
[4] S. Bhattacharya, D. M. Divan, and B. Banerjee, "Synchronous reference harmonic isolator using active series filter," in *Proc. EPE Conf.*, Florence, Italy, 1991, pp. 30–35.
[5] S. Rahmani, N. Mendalek, and K. Al-Haddad, "Experimental design of a nonlinear control technique for three-phase shunt active power filter," *IEEE Trans. Ind. Electron.*, vol. 57, no. 10, pp. 3364–3375, Oct. 2010.
[6] V. Soares, P. Verdelho, and G. D. Marques, "An instantaneous active and reactive current component

method for active filters," *IEEE Trans. Power Electron.*, vol. 15, no. 4, pp. 660–669, Jul. 2000.
[7] R. S. Herrera, P. Salmeron, and K. Hyosung, "Instantaneous reactive power theory applied to active power filter compensation: Different approaches, assessment, and experimental results," *IEEE Trans. Ind. Electron.*, vol. 55, no. 1, pp. 184–196, Jan. 2008.
[8] R. S. Herrera and P. Salmeron, "Instantaneous reactive power theory: A reference in the nonlinear loads compensation," *IEEE Trans. Ind. Electron.*, vol. 56, no. 6, pp. 2015–2022, Jun. 2009.
[9] M. Cirrincione, M. Pucci, G. Vitale, and A. Miraoui, "Current harmonic compensation by a single-phase shunt active power filter controlled by adaptive neural filtering," *IEEE Trans. Ind. Electron.*, vol. 56, no. 8, pp. 3128–3143, Aug. 2009.
[10] J. M. Kanieski, R. Cardoso, H. Pinheiro, and H. A. Gründling, "Kalman filter-based control system for power quality conditioning devices," *IEEE Trans. Ind. Electron.*, vol. 60, no. 11, pp. 5214–5227, Nov. 2013.
[11] S. Buso, L. Malesani, and P. Mattavelli, "Comparison of current control techniques for active filter applications," *IEEE Trans. Ind. Electron.*, vol. 45, no. 5, pp. 722–729, Oct. 1998.
[12] F. Liccardo, P. Marino, and G. Raimondo, "Robust and fast three-phase PLL tracking system," *IEEE Trans. Ind. Electron.*, vol. 58, no. 1, pp. 221–231, Jan. 2011.
[13] C. H. da Silva, R. R. Pereira, L. E. B. da Silva, G. Lambert-Torres, and B. K. Bose, "A digital PLL scheme for three-phase system using modified synchronous reference frame," *IEEE Trans. Ind. Electron.*, vol. 57, no. 11, pp. 3814–3821, Nov. 2010.
[14] K. M. Smedley, L. Zhou, and C. Qiao, "Unified constant-frequency integration control of active power filters—steady-state and dynamics," *IEEE Trans. Power Electron.*, vol. 16, no. 3, pp. 428–436, May 2001.
[15] Q. Chongming and K. M. Smedley, "Three-phase bipolar mode active power filters," *IEEE Trans. Ind. Appl.*, vol. 38, no. 1, pp. 149–158, Jan./Feb. 2002.
[16] Q. Chongming, J. Taotao, and K. M. Smedley, "One-cycle control of three-phase active power filter with vector operation," *IEEE Trans. Ind. Electron.*, vol. 51, no. 2, pp. 455–463, Apr. 2004.
[17] K. Chatterjee, D. V. Ghodke, A. Chandra, and K. Al-Haddad, "Modified one-cycle controlled load compensator," *IET Power Electron.*, vol. 4, no. 4, pp. 481–490, Apr. 2011.
[18] D. V. Ghodke, K. Chatterjee, and B. G. Fernandes, "Modified one-cycle controlled bidirectional high-power-factor ac-to-dc converter,"



IEEE Trans. Ind. Electron., vol. 55, no. 6, pp. 2459–2472, Jun. 2008.

[19] E. S. Sreeraj, K. Chatterjee, and S. Bandyopadhyay, “One cycle controlled single-stage, single-phase voltage sensor-less grid-connected PV system,” IEEE Trans. Ind. Electron., vol. 60, no. 3, pp. 1216–1224, Mar. 2013.

[20] S. Chattopadhyay and V. Ramanarayanan, “Phase-angle balance control for harmonic filtering

of a three-phase shunt active filter system,” IEEE Trans. Ind. Appl., vol. 39, no. 2, pp. 565–574, Mar./Apr. 2003.

[21] E. S. Sreeraj, E. K. Prejith, and K. Chatterjee, “One cycle controlled active harmonic filter,” in Proc IECON, Montreal, QC, Canada, Oct. 25–28, 2012, pp. 621–626

sBibliography



B.HARIKA, Completed B.Tech in Electrical & Electronics Engineering in 2013 from VISHWA BHARATHI INSTITUTE OF TECHNOLOGY & SCIENCES affiliated to JNTUH, Hyderabad and currently pursuing M.Tech in Power Electronics at AVANTHI'S SCIENTIFIC TECHNOLOGICAL & RESEARCH ACADEMY, Gunthapally (V), Hayathnagar (M), R.R.District, Pincode: 501515, Telangana. Area of interest includes Power Electronics. [E-mail:harikareddy375@gmail.com](mailto:harikareddy375@gmail.com)



M.SAIDA RAO He has teaching experience and presently working as Assistant Professor in EEE Dept. at AVANTHI'S SCIENTIFIC TECHNOLOGICAL & RESEARCH ACADEMY, Gunthapally (V), Hayathnagar (M), R.R.District, Pincode: 501515, Telanganastate, India. E-MAIL:- Saidaraomaddineni@gmail.com